27
2/20/79
24 pp DXTIS

MASTER

UCID-18049

Lawrence Livermore Laboratory

TEMPERATURE AND THERMAL STRESS ANALYSIS OF A SWITCHING TUBE ANODE

S. B. SUTTON

JANUARY 1979

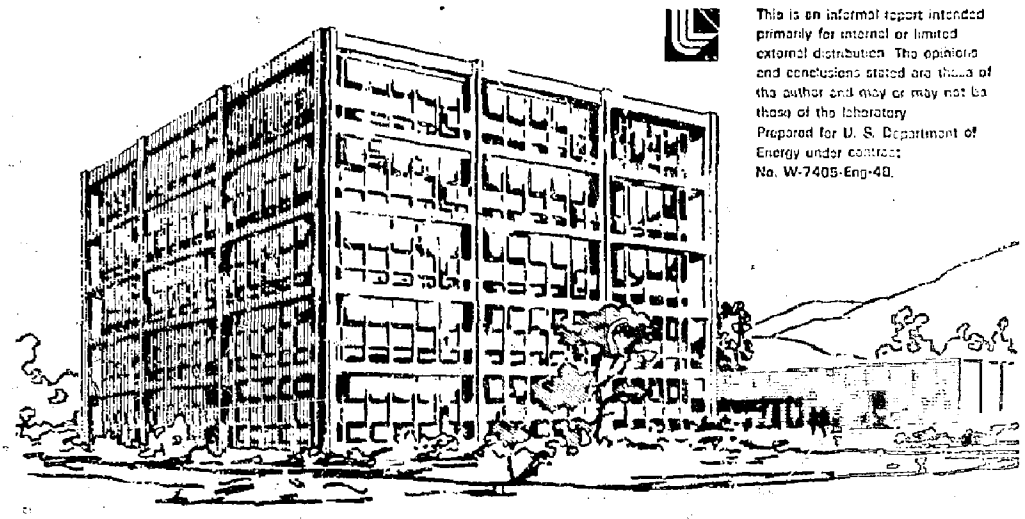

NOMENCLATURE

Bi	Biot Modulus (hL/k)
c	Specific Heat of Metal
E	Young's Modulus
h	Convective Heat Transfer Coefficient
k	Thermal Conductivity of Metal
L	Thickness of Anode
P	Pressure
q	Incident Heat Flux
r	Radius
t	Time
T	Temperature
X	Distance Measured from Inner Surface
θ	Temperature Differential ($T-T_\infty$)
λ	Eigenvalues in Temperature Solution
ν	Poisson's Ratio
α	Thermal Expansion Coefficient
σ	Stress
γ	Thermal Diffusivity ($k/\rho c$)

Subscripts

a	Inner	u	Ultimate
b	Outer	alt	Alternating
r	Radial	eq	Equivalent
z	Axial	∞	Ambient Conditions
θ	Azimuthal		
o	Outside		
s	Average at Steady State		

TEMPERATURE AND THERMAL STRESS ANALYSIS OF A SWITCHING TUBE ANODE

S. B. Sutton

INTRODUCTION

In the design of high power density switching tubes which are subjected to cyclic thermal loads, the temperature induced stresses must be minimized in order to maximize the life expectancy of the tube. Following are details of an analysis performed for the Magnetic Fusion Program at the Lawrence Livermore Laboratory on a proposed tube. The tube configuration is given in Figure 1. The inner surface of the anode is subjected to a bombardment of electrons which transfer their kinetic energy to the copper in the form of a surface heat load. The outer surface is convectively cooled with water to remove this energy from the system. The maximum design heat load is 7.6 MJ/m^2-s applied for 30 seconds. There is approximately a 270 second time span between the end of one pulse and the start of the next. The inner surface is at vacuum pressure while the outer surface is subjected to the static pressure of the cooling water. This causes a compression in the anode prior to thermal loading.

The problem was simplified to one-dimensional approximations for both the thermal and stress analyses. The underlying assumptions and their implications will be discussed in the respective sections of the report.

THERMAL ANALYSIS

For the complete thermal analysis it is necessary to know three quantities: 1) transient temperature behavior, 2) the time it takes the temperature to reach steady state, and 3) the time it takes the anode to cool to its base value after the driving flux is turned off. The method of calculating each of these follows.

Transient Temperature Behavior

Since the ratio of active area length to anode thickness is large (37.5), the heat flow is approximated as one-dimensional over the active area. Actual behavior will deviate from this idealization only at the edges of the active area where the presence of an axial temperature gradient will cause some heat loss in the axial direction. This is neglected in order to maintain the simplified analysis. Further, since the ratio of radius to thickness is large (20.6) curvature of the member is neglected and it is treated as a flat plate.[a] The errors induced by this last assumption will be discussed later.

The simplified geometry is shown in Figure 2. The equation governing one-dimensional heat conduction in a flat plate assuming constant properties is

$$\frac{\partial \theta}{\partial t} = \gamma \frac{\partial^2 \theta}{\partial X^2} \tag{1}$$

where $\gamma = \frac{k}{\rho c}$

$\theta = T - T_\infty$

The boundary condition for the left boundary (X = 0) is the stipulation that the heat flux just inside the surface equal the incident heat flux, i.e.,

$$(q = - k \frac{\partial \theta}{\partial X})_{X=0} \tag{2}$$

while the right boundary (X = L) is a convective condition where

$$(- k \frac{\partial \theta}{\partial X} = h\theta)_{X=L} \tag{3}$$

[a]This simplification allows evaluation of the transient solution on a calculator since the flat plate solution involves cosines while the cylindrical solution involves Bessel Functions.

As an initial condition, the temperature difference is taken as zero ($\theta = 0$).

Using separation of variables, the solution of Equation 1 and the associated boundary conditions and initial condition is

$$\frac{\theta}{q} = \left[\frac{L-X}{k} + \frac{1}{h}\right] + \sum_{n=1}^{\infty} A_n e^{-\gamma\lambda_n^2 t} \cos \lambda_n X \tag{4}$$

where $$A_n = \frac{-1}{\lambda_n} \frac{\left\{\frac{1}{h} \sin\lambda_n L + \frac{1}{k\lambda_n}(1 - \cos\lambda_n L)\right\}}{(\lambda/2 + \frac{1}{4\lambda_n} \sin\lambda_n L)} \tag{5}$$

and the eigen values are the roots of the transcendental equation.

$$\lambda_n \tan\lambda_n L = \frac{h}{k} \tag{6}$$

It is noted that the first part of the expression represents the steady-state solution to Equation 1, while the series portion is a transient correction.

To assess the effect of neglecting curvature, the steady-state cylindrical solution is considered. The governing equation is

$$\frac{d}{dr}\left(r\frac{d\theta}{dr}\right) = 0 \tag{7}$$

with the accompanying boundary conditions

$$\left(q = -k \frac{d\theta}{dr}\right)_{r = r_a} \tag{8}$$

$$\left(-k \frac{d\theta}{dr} = h\theta\right)_{r = r_b} . \tag{9}$$

The solution to this system of equations is

$$\frac{\theta}{q} = -\frac{r_a}{k} \ln \frac{r}{r_b} + \frac{r_a}{hr_b} \tag{10}$$

A comment is made in the results section of this report on the difference between the planar and cylindrical solutions.

Time to Reach Steady-State

For an estimate of the time it takes for the anode to reach the steady elevated temperature, consider Equation 4 with only one term from the series.[a]

$$\frac{\theta}{q} = \left[\frac{L-X}{k} + \frac{1}{h}\right] + A_1 e^{-\gamma\lambda_1^2 t} \cos\lambda_1 X \tag{11}$$

If we use the inner surface ($X = 0$) as a basis, then the time it takes for the temperature to reach a percentage (δ) of the steady value is given by

$$t = \frac{1}{\gamma\lambda_1^2} \ln\left\{\frac{A_1}{(\delta-1)\left[\frac{L}{k} + \frac{1}{h}\right]}\right\} \tag{12}$$

Time to Cool-Down

To estimate the cool-down time, consider the case where the internal resistance is negligible ($B_i = \frac{hL}{k} < .1$). For this condition the average temperature in the body is given by

$$\theta = \theta_s e^{-\frac{h\gamma t}{kL}} \quad . \tag{13}$$

Thus, the time it takes for the temperature to be reduced to a percentage

[a] The author has found this to be a very reasonable estimate since the influence of the higher order terms has been found to be less than 15% of the first term.

(δ) of the steady value is given by

$$t = \frac{kL}{ha} \ln\left(\frac{1}{\delta}\right) \tag{14}$$

The limitations of this analysis are discussed in a later section.

STRESS ANALYSIS

Since details of any structural confinement of the anode were unavailable at the time of this analysis, it is assumed that it is free to radially expand, and that axial expansion is free so there is no net force in the axial direction. It is further assumed that the thermal response time of the anode is long compared to the structural response time so that an equilibrium condition exists at all times. In addition, curvature effects are included.

In this analysis two types of stresses are considered: a) those of thermal origin and b) compressive stresses caused by the pressure differential across the anode. A discussion of the method of calculating each is given. Finally, a discussion of the method for estimating fatigue life is given. The stress orientations are shown in Figure 3.

Thermal Stress

The solution to this problem is [1]

$$\sigma_r = \frac{\alpha E}{1-\nu} \frac{1}{r^2} \left(\frac{r^2 - r_a^2}{r_b^2 - r_a^2} \int_{r_a}^{r_b} \theta r dr - \int_{r_a}^{r} \theta r dr \right) \tag{15}$$

$$\sigma_\theta = \frac{\alpha E}{1-\nu} \frac{1}{r^2} \left(\frac{r^2 - r_a^2}{r_b^2 - r_a^2} \int_{r_a}^{r_b} \theta r dr + \int_{r_a}^{r} \theta r dr - \theta r^2 \right) \tag{16}$$

$$\sigma_Z = \frac{\alpha E}{1-\nu} \left(\frac{2}{r_b^2 - r_a^2} \int_{r_a}^{r_b} \theta r dr - \theta \right) . \tag{17}$$

Noting that $r = r_a + X$; upon substitution of Equation 4 these expressions integrate to

$$\frac{\sigma_r}{q} = \frac{\alpha E}{1-\nu}\left(\frac{1}{(X+r_a)^2}\right)\left\{\frac{X^2+2r_aX}{L^2+2r_aL}\left[L\left(\frac{L}{k}+\frac{1}{h}\right)\left(r_a+\frac{L}{2}\right)-\frac{L^2}{k}\left(\frac{r_a}{2}+\frac{L}{3}\right)\right.\right.$$

$$+\sum_{n=1}^{\infty} A_n e^{-\gamma\lambda_n^2 t}\left(\frac{r_a}{\lambda_n}\sin\lambda_n L+\frac{1}{\lambda_n^2}\cos\lambda_n L+\frac{L}{\lambda_n}\sin\lambda_n L\right.$$

$$\left.\left.-\frac{1}{\lambda_n^2}\right)\right]-\left[X\left(\frac{L}{k}+\frac{1}{h}\right)\left(r_a+\frac{X}{2}\right)-\frac{X^2}{k}\left(\frac{r_a}{2}+\frac{X}{3}\right)\right.$$

$$+\sum_{n=1}^{\infty} A_n e^{-\gamma\lambda_n^2 t}\left(\frac{r_a}{\lambda_n}\sin\lambda_n X+\frac{1}{\lambda_n^2}\cos\lambda_n X\right.$$

$$\left.\left.+\frac{L}{\lambda_n}\sin\lambda n X-\frac{1}{\lambda_n^2}\right)\right]\Bigg\} \qquad (18)$$

$$\frac{\sigma_\theta}{q} = \frac{\alpha E}{1-}\ \frac{1}{(X+r_a)^2}\ \left\{\frac{X^2+2r_aX+2r_a^2}{L^2+2r_aL}\ \left[L\left(\frac{L}{k}+\frac{1}{h}\right)\left(r_a+\frac{L}{2}\right)\right.\right.$$

$$-\frac{L^2}{k}\left(\frac{r_a}{2}+\frac{L}{3}\right)+\sum_{n=1}^{\infty} A_n e^{-\gamma\lambda_n^2 t}\left(\frac{r_a}{\lambda_n}\sin\lambda_n L\right.$$

$$\left.\left.+\frac{1}{\lambda_n^2}\cos\lambda_n L+\frac{L}{\lambda_n}\sin\lambda_n L-\frac{1}{\lambda_n^2}\right)\right]+\left[X\left(\frac{L}{k}+\frac{1}{h}\right)\left(r_a+\frac{X}{2}\right)\right.$$

$$-X^2\left(\frac{r_a}{2}+\frac{X}{3}\right)-\left(\frac{L-X}{k}+\frac{1}{h}\right)(r_a+X)^2$$

$$+\sum_{n=1}^{\infty} A_n e^{-\gamma\lambda_n^2 t}\left(\frac{r_a}{\lambda_n}\sin\lambda_n X\right.$$

$$\left.\left.+\frac{1}{\lambda_n^2}\cos\lambda_n x+\frac{L}{\lambda_n}\sin\lambda_n X-\frac{1}{\lambda_n^2}-(r_a+X)^2\right)\right]\Bigg\} \qquad (19)$$

$$\frac{\sigma_z}{q} = \frac{\alpha E}{1-\nu}\left\{\frac{2}{L^2 + 2r_a L}\left[L\left(\frac{L}{k} + \frac{1}{h}\right)\left(r_a + \frac{L}{2}\right) - \frac{L^2}{2}\left(r_a + \frac{L}{3}\right)\right.\right.$$

$$+ \sum_{n=1}^{\infty} A_n e^{-\gamma\lambda_n^2 t}\left(\frac{r_a}{\lambda_n}\sin\lambda_n L + \frac{1}{\lambda_n^2}\cos\lambda_n L + \frac{L}{\lambda_n}\sin\lambda_n L\right.$$

$$\left.\left. - \frac{1}{\lambda_n^2}\right)\right] - \left[\frac{L-X}{k} + \frac{1}{h} + \sum_{n=1}^{\infty} A_n e^{-\gamma\lambda_n^2}\cos\lambda_n x\right]\Bigg\} \qquad (20)$$

As a limiting condition, consider the steady-state case of a very thin cylinder ($L << r_a$). Noting that the maximum compressive stress[a] occurs at the inner surface and that the maximum tensile stress occurs at the outer surface, the expression for σ_θ reduces to

inner surface: $$\frac{\sigma_\theta}{q} = \frac{-\alpha E}{2(1-\nu)}\frac{L}{k} \qquad (21)$$

outer surface: $$\frac{\sigma_\theta}{q} = \frac{\alpha E}{2(1-\nu)}\frac{L}{k} \qquad (22)$$

It is important to note that the quantity qL/k is the temperature difference across the anode. Thus, the limiting steady state stress values depend only on the temperature difference and not on the temperature value.

Pressure Induced Stress

Due to the pressure differential that exists across the anode, a compressive pre-stress is established. These stresses for a cylinder with vacuum on the inner surface are given by [1]

[a]The maximum stresses will always be in the θ direction.

$$\frac{\sigma_r}{P_o} = \left[\frac{r_a^2 r_b^2}{r_b^2 - r_a^2}\right]\frac{1}{r^2} - \frac{r_b^2}{r_b^2 - r_a^2} \tag{23}$$

$$\frac{\sigma_\theta}{P_o} = -\left[\frac{r_a^2 r_b^2}{r_b^2 - r_a^2}\right]\frac{1}{r^2} - \frac{r_b^2}{r_b^2 - r_a^2} \tag{24}$$

These stresses are superimposed on the thermal stresses at all times.

Fatigue Life Determination

For fatigue purposes, only tensile stresses must be considered. Thus, the outer surface of the anode is of primary interest. It should be noted however, that the inner boundary compressive stress must be evaluated to determine if it exceeds the yield limit.

In this system, the outer boundary stress cycles about a mean stress other than zero, as depicted in Figure 4. For this situation the ASME Boiler and Pressure Vessel Code[2] recommends that the tensile stress to be used in the S-N curve for fatigue analysis is given by[b]

$$\sigma_{eq} = \left[\frac{\sigma_{alt}}{1 - \frac{\sigma_{mean}}{\sigma_u}}\right]\beta \tag{25}$$

[b] β is a contingency factor. The recommended value is 1.2 [3].

where:

If $\sigma_{alt} + \sigma'_{mean} \leq \sigma_y$; $\sigma_{mean} = \sigma'_{mean}$

If $\sigma_{alt} + \sigma'_{mean} > \sigma_y$

and $\sigma_{alt} < \sigma_y$; $\sigma_{mean} = \sigma_y - \sigma_{alt}$

If $\sigma_{alt} \geq \sigma_y$; $\sigma_{mean} = 0$

PROPERTIES

The thermal and mechanical properties for OFHC copper are given in Table I, while the S-N curve is given in Figure 5.

In addition, it is necessary to estimate a value for the convective heat transfer coefficient at the outer surface of the anode. It must be recognized that depending on the heat flux value, the transfer mechanism will either be forced convection with water or forced convection with surface boiling. The convective surface is not flat. It is known to be composed of semi-circular slots running the length of the anode and also in a spiral fashion around it. However, since details of the configuration were unavailable, an accurate prediction of the non-boiling coefficient could not be made. For purposes of this study the non-boiling coefficient was bounded using the suggestion of Kreith [6] who states that

$$h = 300 - 12000 \text{ J/m}^2\text{s K}$$
$$(50 - 2000 \text{ BTU/ft}^2\text{hr°F})$$

The coefficient for nucleate boiling with forced convection is estimated using the results of McAdams [7], as given in Figure 6. From this curve, the convective transfer coefficient can be estimated if the saturation temperature of the fluid is known. It is important to note that this boiling coefficient will always be much larger than the coefficient where boiling is not present.

RESULTS

The discussion of results is divided into four sections: 1) heat-up and cool-down times, 2) temperature response, 3) stress evaluation, and 4) fatigue life.

Heat-Up and Cool-Down Times

It is important to determine if a steady-state solution is reached during the 30 sec duration of the heat flux. This is estimated using Equation 12. Estimates of heating time to 90% and 95% of the steady value are given in Figure 7 as a function of the convection coefficient. We thus see that for large convection coefficients (>5000 J/m^2s)[a] the anode will be in a steady-state condition for the vast majority of the flux time.

Likewise it is important to estimate the cool-down time to determine if the body can equilibrate with the water before the application of the next pulse. Estimates of the cool-down time, using Equation 13, are given in Figure 8. It should be noted that Equation 13 is ideally valid only for values of the convection coefficient less than 7000 J/m^2s K. However, since the cool-down times for all large values of the convection coefficient (>5000 J/m^2s K) are small compared to the 270 seconds between pulses, the numbers indicate that the anode has more than sufficient time to equilibrate at the base temperature before the application of the next pulse.

Performing the complete transient analysis indicated that the maximum temperature difference across the anode will exist at steady-state and thus the maximum stresses will be expected to exist at steady-state. The majority of the remaining discussion will concentrate on the steady state results.

---

[a]Later discussion will indicate that very large coefficient values are to be expected in this system.

Temperature Response

Figure 9 gives the relationship between temperature rises at the left (X=0) and right (X=L) surfaces and the heat transfer coefficient. Consider the situation where the heat flux is 7.6 M J/m^2-s (maximum design limit) and the convection coefficient is 12000 J/m^2-s K (maximum value for forced convection without nucleate boiling). For these conditions, the temperature rise at the convection boundary is approximately 450°K. This clearly violates the no boiling assumption since nucleate boiling will occur whenever the surface temperature exceeds the saturation temperature. Boiling can be expected down to a flux that is 20% of the maximum design. On this basis, the remaining discussion assumes the existence of nucleate boiling at the outer surface and appropriate convection coefficient were evaluated using Figure 6.

The above is based on the planar analysis. Results for the cylindrical analysis differed by less than 3%, thus verifying the suitability of the planar approach.

Figure 10 gives the steady-state temperature rises at the inner and outer surfaces vs. incident heat flux for various values of the fluid pressure (or saturation temperature). It will be noted that for the maximum design flux (7.6 MJ/m^2-s) the outer surface temperature rise varies from 145 to 175°K, while the average body temperature rise varies from 210 to 245°K.

Stress Evaluation

Performing the complete transient analysis indicated that the maximum stresses will occur at steady state.

Calculation of stresses using the large time form of Equation 19 and limiting Equations 21 and 22 indicated the curvature effects could indeed be neglected since the difference in stress is less than 3%. Using the limiting Equations 21 and 22, Figure 11 gives the temperature differential and surface stresses as a function of the incident heat flux. For the maximum flux of 7.6 MJ/m^2-s, the temperature differential is slightly greater than 100°K and the stress is approximately 155 MPa (22500 psi).

The compressive stresses induced by the pressure differential across the anode are given in Figure 12. It is important to note that this pre-compression is generally negligible compared to the thermal stress for heat fluxes greater than 5 MJ/m^2s.

Fatigue Life

Figure 13 gives the projected cycle fatigue limit versus heat flux using Figures 5, 11 and 12 and Equation 25. It was found that the pressure induced stress influenced the equivalent stress by less than 2%. The 200°C temperature curve in Figure 5 was used since the outer surface temperature will rise to less than 202°C on the spatial average. It is interesting to note how flat the curve is for this system. Under these conditions, fatigue can be regarded as nearly a threshold phenomenon.

CONCLUSIONS

On the basis of this analysis the following conclusions can be made:

1. Nucleate boiling at the outer surface will likely exist for driving heat fluxes greater than 1.5 MJ/m^2s.
2. Heat-up and cool-down times are small compared to the pulse length.
3. The outer surface temperature rise may be as much as 175°K.
4. The thermally induced tensile stress at the outer surface may be as much as 155 MPa (22,500 psi).
5. The pressure induced compressive stresses will generally be small compared to the thermal stress.
6. For long life performance, ($>10^6$ cycles) the flux should probably not exceed 50% of the maximum design limit.
7. Because of the flatness of the fatigue life curve, testing must be performed to assure long life behavior.

REFERENCES

1. S. P. Timoshenko, "Theory of Elasticity," McGraw-Hill, New York (1970).

2. "Criteria of the ASME Boiler and Pressure Vessel Code for Design by Analysis in Sections III and VIII, Division 2," ASME, New York (1969).

3. T. Baumeister, "Mark's Standford Handbook for Mechanical Engineers," McGraw-Hill, New York (1978).

4. RCA Report to LLL, October 16, 1978.

5. F. Kreith, "Principles of Heat Transfer," International Textbook, Scranton, PA (1968)

6. W. H. McAdams, et al., "Heat Transfer at High Rates to Water with Surface Boiling," Ind. Eng. Chem., Vol. 41, 1945.

TABLE I

THERMAL AND MECHANICAL PROPERTIES OF OFHC COPPER [4]

	Engineering Units	SI Units
Density (ρ)	558 lb/ft^3	8.95 Mg/m^3
Specific Heat (c)		381 J/kg K
Thermal Conductivity (k)	226 BTU/hr.ft°F	391 J/smK
Poissons Ratio (ν)	.35	.35
Elastic Modulus (E)	16x10^6 psi	110 GPa
Thermal Expansion Coefficient (α)	9.8 x 10^{-6}/°F	1.8 x 10^{-5}/ K
Yield Strengtn	45 x 10^3 psi	310 MPa
Tensile Strength	50 x 10^3 psi	350 MPa

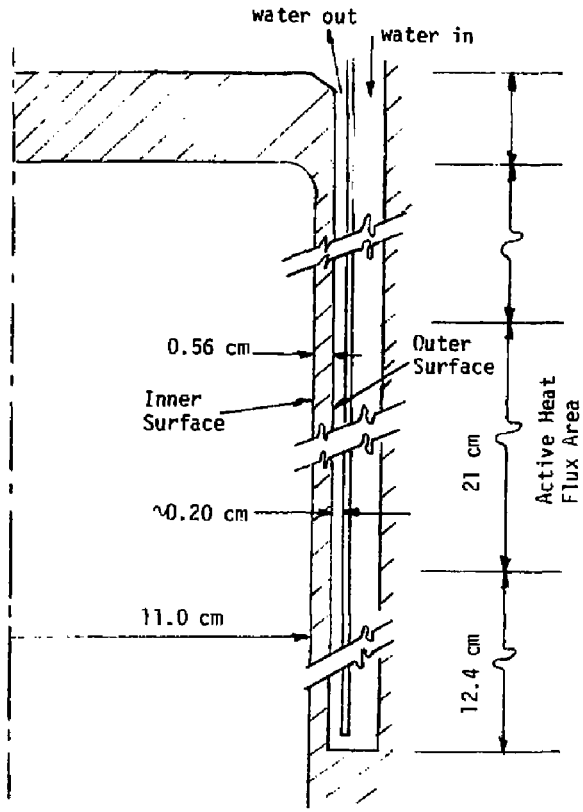

FIGURE 1. Anode Configuration

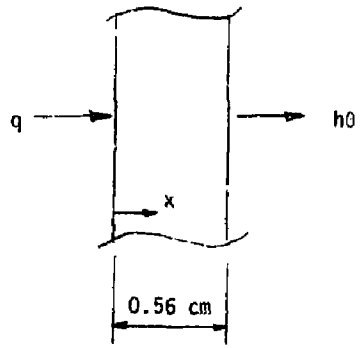

FIGURE 2. Idealization for Thermal Analysis

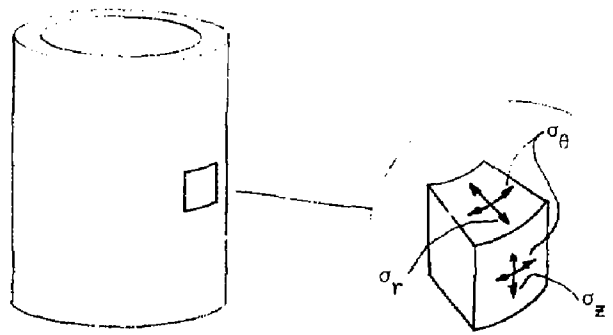

FIGURE 3. Stress Nomenclature

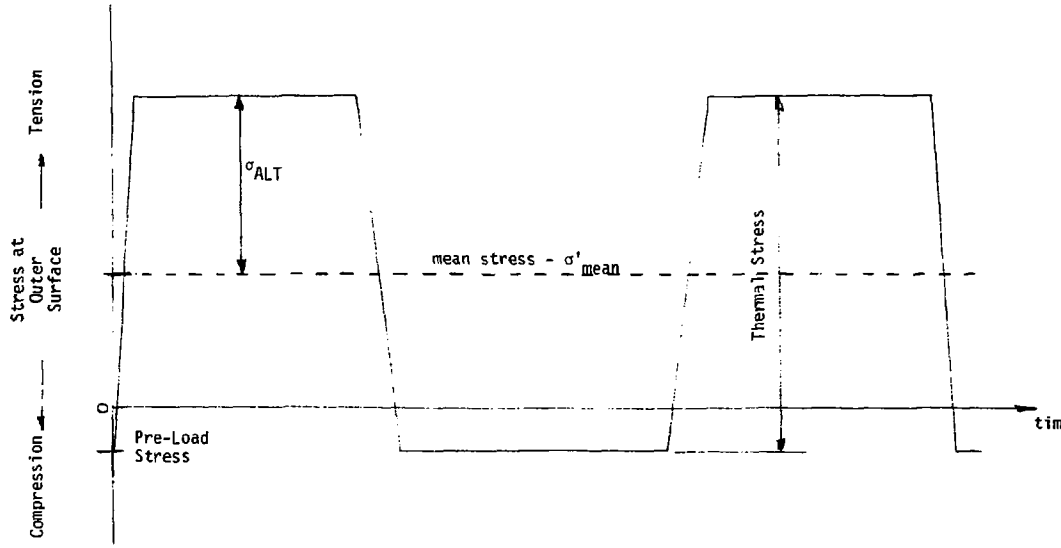

FIGURE 4. Depiction of Stress Behavior at Outer Boundary of Cylinder

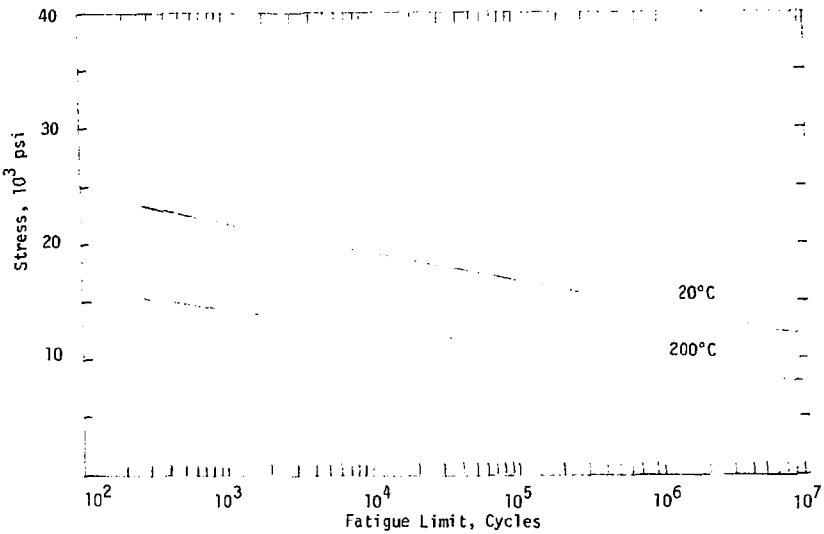

FIGURE 5. S-N Curve for OFHC Copper [5].

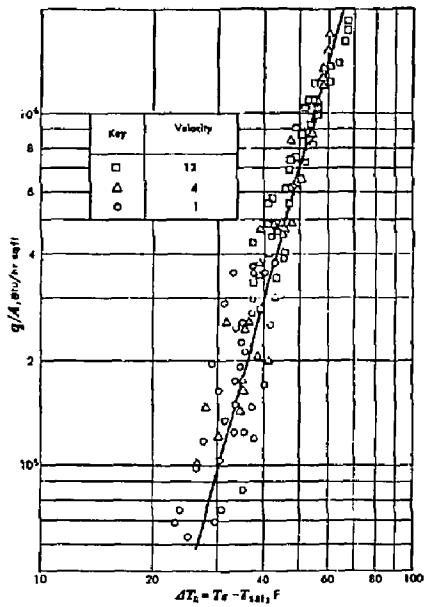

FIGURE 6. Relationship of Excess Temperature to Heat Flux for Nucleate Surface Boiling

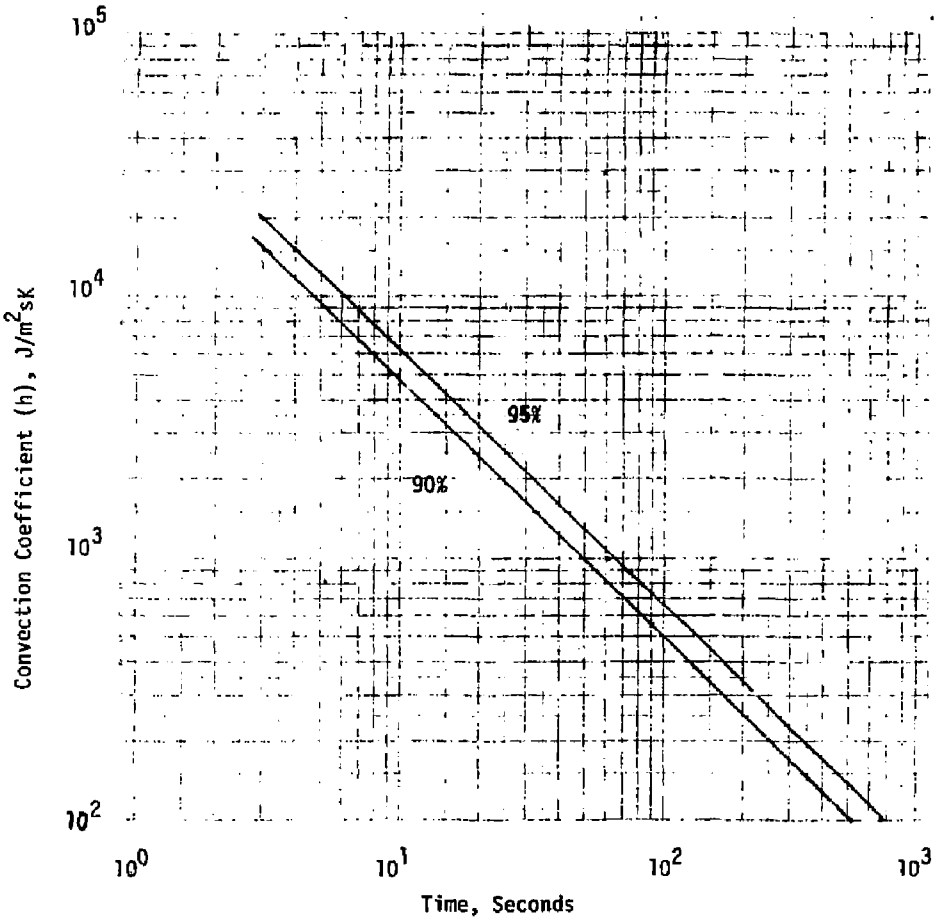

FIGURE 7. Estimate of Heat-Up Time

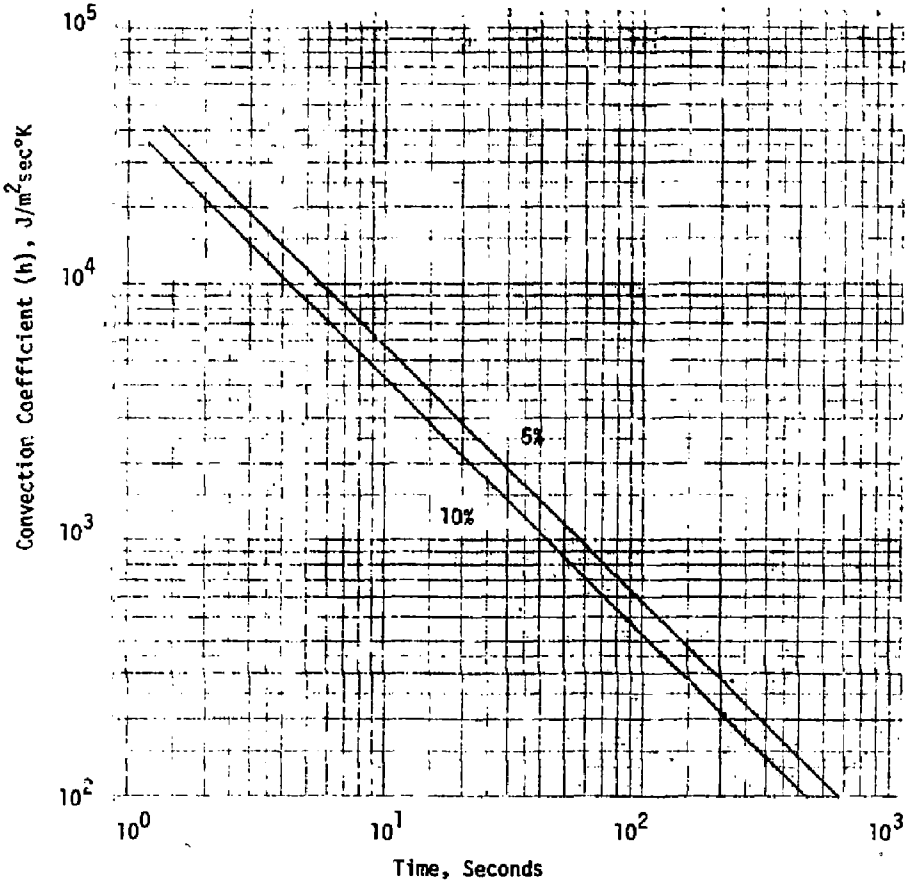

FIGURE 8. Estimate of Cool-Down Time

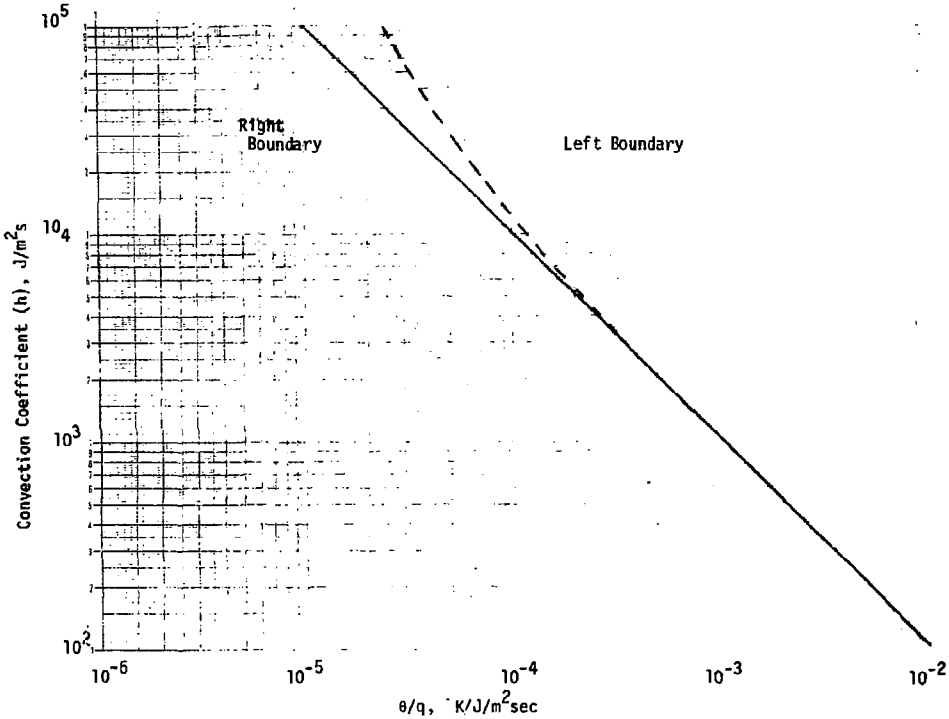

FIGURE 9. Steady-State Surface Temperature Behavior in the Absence of Boiling

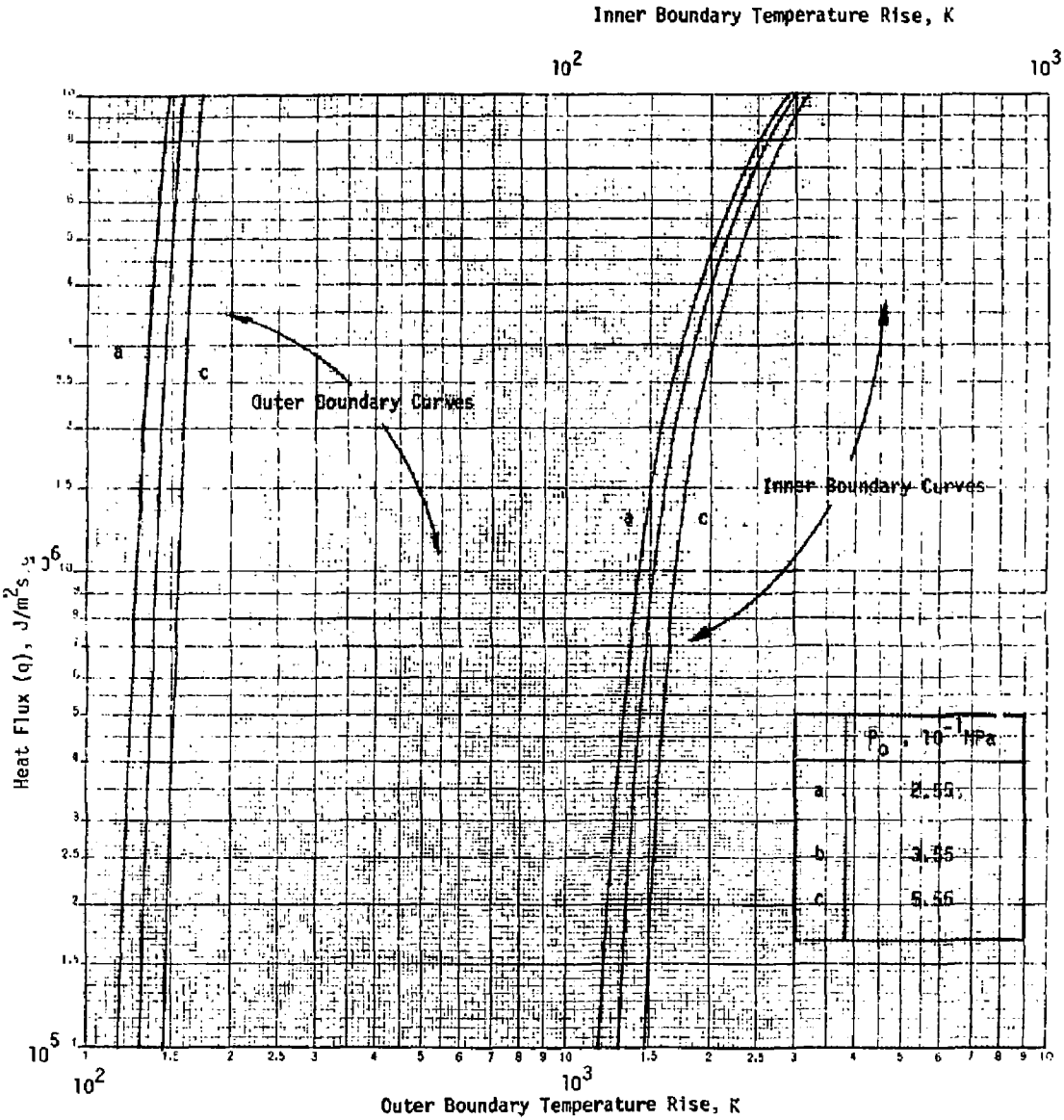

FIGURE 10. Surface Temperature Rises at Steady-State Assuming Boiling Heat Transfer

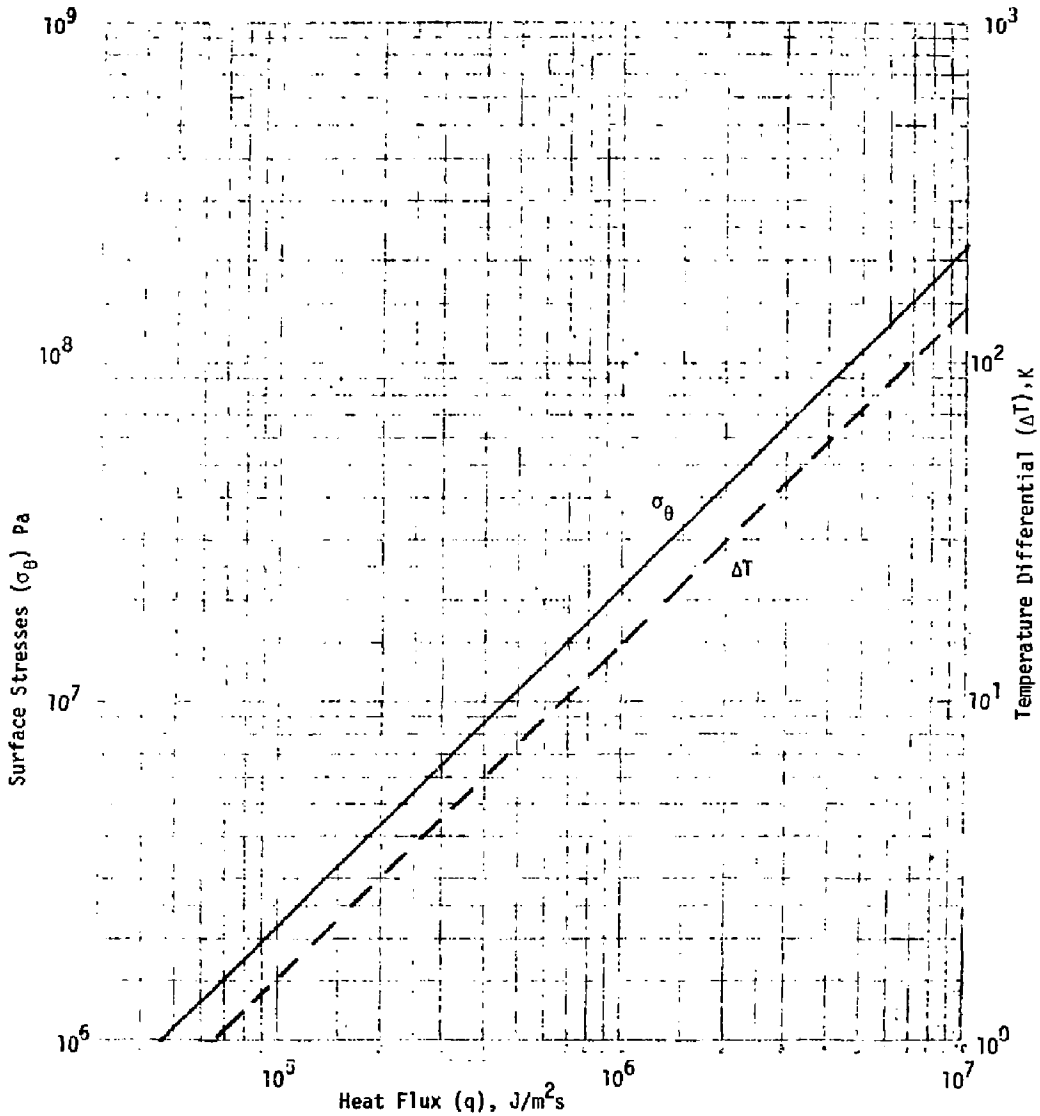

FIGURE 11. Relationship of Surface Stress and Differential Temperatures to Heat Flux

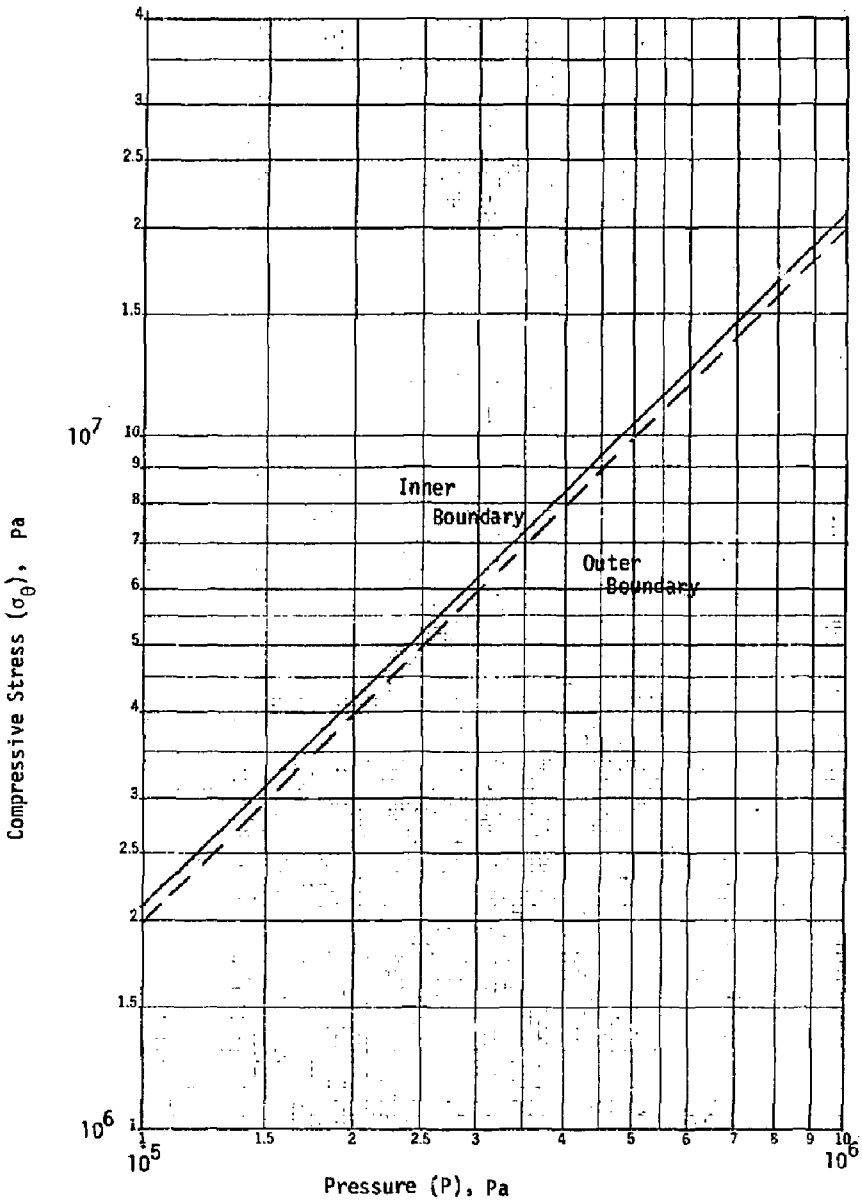

FIGURE 12. Pressure Induced Stresses

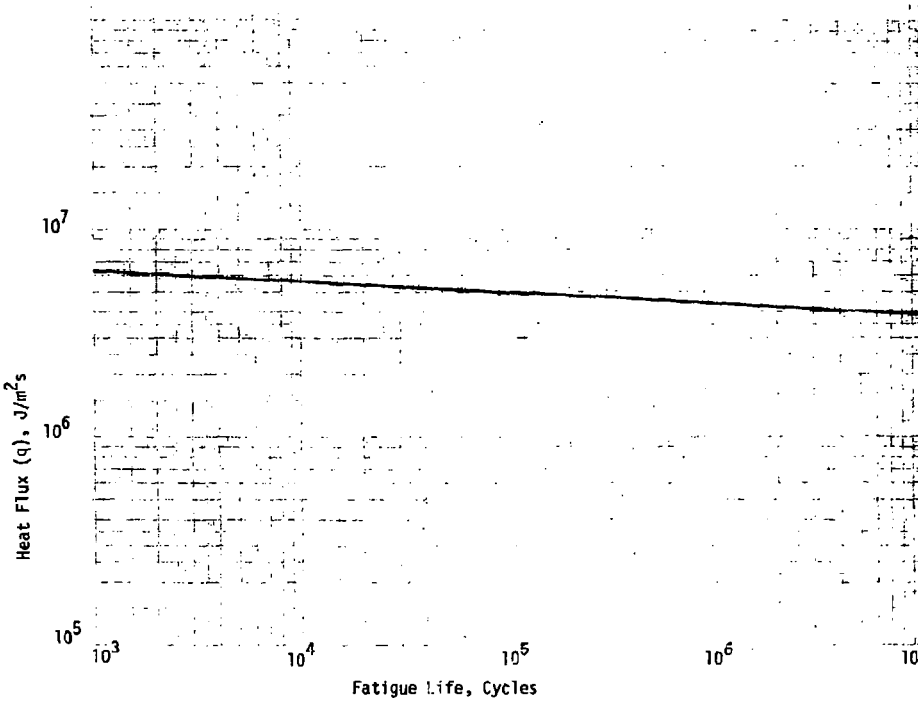

FIGURE 13. Estimate of Fatigue Life as a Function of Heat Flux.